Developmental Cell
Article

Cthrc1 Selectively Activates the Planar Cell Polarity Pathway of Wnt Signaling by Stabilizing the Wnt-Receptor Complex

Shinji Yamamoto,[1] Osamu Nishimura,[2] Kazuyo Misaki,[3] Michiru Nishita,[4] Yasuhiro Minami,[4] Shigenobu Yonemura,[3] Hiroshi Tarui,[2] and Hiroshi Sasaki[1,*]
[1]Laboratory for Embryonic Induction
[2]Genome Resource and Analysis Unit
[3]Laboratory for Cellular Morphogenesis
RIKEN Center for Developmental Biology, 2-2-3 Minatojima-minamimachi, Chuo-ku, Kobe, Hyogo 650-0047, Japan
[4]Department of Physiology and Cell Biology, Faculty of Medical Sciences, Graduate School of Medicine, Kobe University, Chuo-ku, Kobe, Hyogo 650-0017, Japan
*Correspondence: sasaki@cdb.riken.jp
DOI 10.1016/j.devcel.2008.05.007

SUMMARY

Vertebrate Wnt proteins activate several distinct pathways. Intrinsic differences among Wnt ligands and Frizzled (Fzd) receptors, and the availability of pathway-specific coreceptors, LRP5/6, and Ror2, affect pathway selection. Here, we show that a secreted glycoprotein, Cthrc1, is involved in selective activation of the planar cell polarity (PCP) pathway by Wnt proteins. Although *Cthrc1* null mutant mice appeared normal, the introduction of a heterozygous mutation of a PCP gene, *Vangl2*, resulted in abnormalities characteristic of PCP mutants. In HEK293T cells, Cthrc1 activated the PCP pathway but suppressed the canonical pathway. Cell-surface-anchored Cthrc1 bound to Wnt proteins, Fzd proteins, and Ror2 and enhanced the interaction of Wnt proteins and Fzd/Ror2 by forming the Cthrc1-Wnt-Fzd/Ror2 complex. Consistent with this, Ror2 mutant mice also showed PCP-related abnormalities in the inner ear. These results suggest that Cthrc1 is a Wnt cofactor protein that selectively activates the Wnt/PCP pathway by stabilizing ligand-receptor interaction.

INTRODUCTION

Wnt proteins are members of a family of secreted signaling molecules that have multiple roles in the development of the organism throughout the animal kingdom. In vertebrates, Wnt proteins play central roles in regulation of body-axis specification, patterning of germ layers and tissues, differentiation and proliferation of stem/progenitor cells, morphogenetic movements during embryogenesis and organogenesis, and growth and metastasis of cancers/tumors. At the cellular level, such multifunctionality of Wnt signaling is achieved through the activation of different intracellular signaling pathways (Logan and Nusse, 2004; Veeman et al., 2003a).

The best-characterized pathway is the canonical Wnt pathway, which leads to the stabilization of β-catenin proteins (Logan and Nusse, 2004). An increase in the β-catenin level leads to its translocation to the nucleus, where it interacts with TCF/LEF-family transcription factors to activate the expression of target genes. During vertebrate development, canonical Wnt signaling is involved in determining cell fate and the regulation of growth, including formation of the body axis, patterning of the neuroectoderm, and amplification of neural progenitors. The noncanonical pathway is further classified into two subsidiary pathways: Wnt/planar cell polarity (PCP) and Wnt/Ca^{2+} (Habas and Dawid, 2005). The downstream components of the Wnt/PCP pathway resemble those of PCP signaling in *Drosophila.* The Wnt/PCP pathway promotes activation of small GTPases, including RhoA and Rac1, and their downstream protein kinases, ROCK and JNK, respectively, to regulate actin polymerization. In vertebrates, Wnt/PCP signaling plays important roles in morphogenetic processes, including convergent-extension movements during gastrulation and the alignment of the ciliary bundle of the sensory hair cells of the organ of Corti. In contrast, the Wnt/Ca^{2+} pathway is characterized to a lesser extent. It promotes the intracellular increase in Ca^{2+} concentration and activates Ca^{2+}-sensitive enzymes such as PKC, CamKII, and calcineurin.

A detailed mechanism of the selective activation of certain signaling pathways by Wnt proteins is not known. Vertebrate Wnt proteins have been classified into two groups (Shimizu et al., 1997; Slusarski et al., 1997). One group, including Wnt1, Wnt3a, and Wnt8, contain Wnt proteins often referred to as "canonical Wnt proteins"; they stimulate the canonical Wnt pathway, whereas Wnt5a and Wnt11 are classified as "noncanonical Wnt proteins." Such differential activities indicate that pathway selection depends on the intrinsic nature of Wnt proteins. In contrast to these observations, the relationships between Wnt proteins and pathways are not strictly maintained in cultured cells (Kishida et al., 2004; Mikels and Nusse, 2006), indicating that pathway selection by Wnt proteins depends on the cellular context. Wnt proteins use Frizzled (Fzd) receptors and pathway-specific coreceptors for signaling. LRP5 and LRP6 are coreceptors for the canonical pathway (Pinson et al., 2000; Tamai et al.,

2000), whereas Ror2 is a coreceptor for the noncanonical pathway (Hikasa et al., 2002; Oishi et al., 2003). The availability of these coreceptors also affects pathway selection by Wnt proteins (Mikels and Nusse, 2006).

In the present work, we found that the protein collagen triple helix repeat containing 1 (Cthrc1) is involved in the selective activation of the PCP pathway by Wnt proteins. *Cthrc1* was originally identified as an overexpressed gene in injured rat arteries, and it encodes a secreted glycoprotein with 12 repeats of the GXY motif, which is characteristic of collagens (Pyagay et al., 2005). Cthrc1 increases cellular motility to repair the injury by limiting the deposition of collagen matrix and promoting cell migration (Pyagay et al., 2005). Aberrant expression of *Cthrc1* is also observed in some metastatic melanoma cells (Tang et al., 2006). Therefore, Cthrc1 is considered to be a promigratory protein.

Here, we examined the role of the *Cthrc1* gene during development in the mouse. *Cthrc1* null mutants did not exhibit obvious abnormalities, but introduction of a heterozygous mutation of a PCP gene, *vang-like 2* (*Vangl2*), into this mutant background ($Cthrc1^{LacZ/LacZ}$;$Vangl2^{Lp/+}$) resulted in clear PCP phenotypes. In HEK293T cells, Cthrc1 activated the PCP pathway by promoting the formation of a ligand-receptor complex for the Wnt/PCP pathway (Wnt-Fzd/Ror2) regardless of the class of Wnt protein. The results now available indicate that Cthrc1 is a Wnt signaling component that selectively activates the PCP pathway, and that its underlying mechanism is enhancement of the Wnt-receptor interaction by forming a stabilized Cthrc1-Wnt-Fzd/Ror2 complex.

RESULTS

Expression of *Cthrc1* in Tissues in Which the PCP Signal Is Active

To identify the novel genes expressed in the node and the notochord, we generated a single-cell cDNA library of the node/notochord cell of embryonic day (E) 8.5 mouse embryos and performed in situ hybridization screening. This screening identified *Cthrc1* as a gene specifically expressed in the node and the notochord. No signal was observed at E6.5 (Figure 1A). Concomitant with node formation, *Cthrc1* expression was initiated in the node at E7.5 and was extended anteriorly to the notochord (Figures 1B and 1C). At the later stages, *Cthrc1* was also expressed in other tissues, as reported previously (Durmus et al., 2006). At E9.5, *Cthrc1* was detected in the ventral midline of the midbrain, dorsal hindbrain, and otic vesicle, as well as the posterior notochord (Figure 1D). At E18.5, *Cthrc1* was also expressed in the sensory hair cells of the inner ear, including the crista, utricle, and cochlea (organ of Corti) (Figures 1E–1H). Because of the similarities between the expression patterns of *Cthrc1* and the adjacent gene, *Fzd6*, which is involved in PCP signaling (Wang et al., 2006b), we hypothesized that *Cthrc1* is involved in PCP signaling.

Exencephaly and Misorientation of Cochlear Sensory Hair Cells in $Cthrc1^{LacZ/LacZ}$;$Vangl2^{Lp/+}$ Mice

To reveal the in vivo function of *Cthrc1*, we generated *Cthrc1* mutant mice by replacing the first exon with a *LacZ* gene by using homologous recombination in embryonic stem (ES) cells

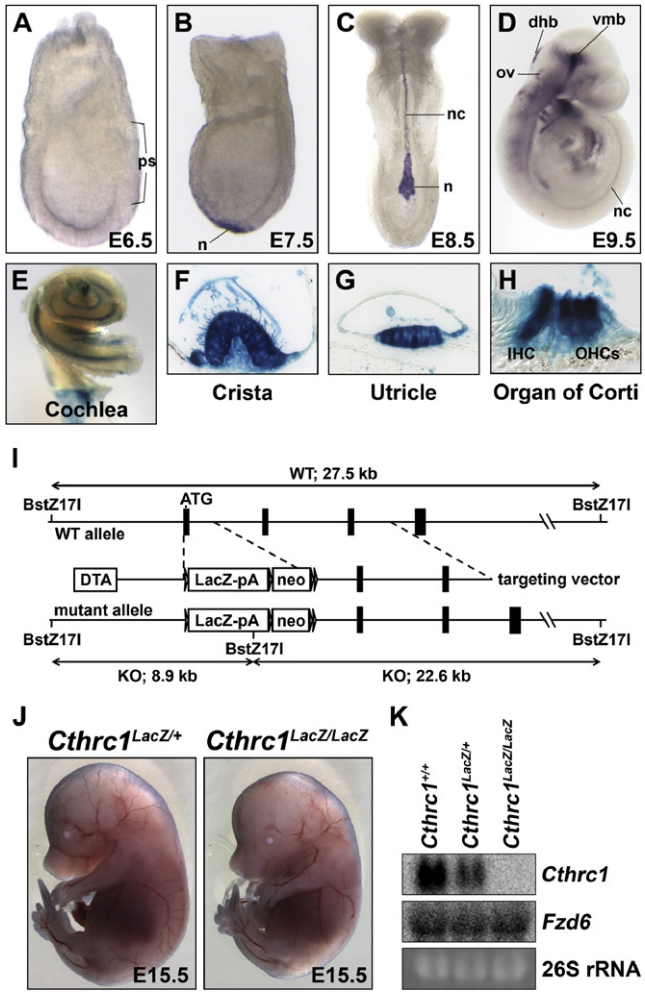

Figure 1. Expression of *Cthrc1* and Production of *Cthrc1* Mutant Mice

(A–D) Whole-mount in situ hybridization showing expression of *Cthrc1* in embryos from E6.5 to E9.5.

(E–H) β-Galactosidase activity staining of $Cthrc1^{LacZ/+}$ embryos showing the expression of *Cthrc1* in the E18.5 inner ear. *Cthrc1* is expressed in the (H) organ of Corti, (E) cochlea, (F) crista, and (G) utricle.

(I) Targeting strategy of the *Cthrc1* locus. A cassette consisting of *LacZ*-pA and *PGK-neo*-pA (neo) was introduced upstream of the translation initiation codon together with deletion of coding sequences encoded by exon 1.

(J) External morphology of E15.5 $Cthrc1^{LacZ/+}$ and $Cthrc1^{LacZ/LacZ}$ embryos.

(K) Northern blot hybridization of E9.5 RNA. Ten micrograms of total RNA was used for each sample. ps, primitive streak; n, node; nc, notochord; vmb, ventral midbrain; dhb, dorsal hindbrain; ov, otic vesicle.

(Figure 1I). $Cthrc1^{LacZ/+}$ mice were apparently normal, and the intercross of $Cthrc1^{LacZ/+}$ mice produced $Cthrc1^{LacZ/LacZ}$ mice, which did not show any obvious abnormalities and were fertile (Figure 1J and data not shown). Northern blot analysis of E9.5 embryos confirmed the absence of *Cthrc1* transcripts in $Cthrc1^{LacZ/LacZ}$ embryos (Figure 1K), indicating the null mutation of *Cthrc1*. Expression of the adjacent gene, *Fzd6*, was not affected (Figure 1K). The absence of clear abnormalities in *Cthrc1* mutants prompted us to further test our hypothesis by introducing a heterozygous mutation of the PCP gene *Vangl2*. *Vangl2* is

a homolog of the *Drosophila* PCP gene *Van Gogh/Strabismus* and encodes a four-transmembrane protein with a PDZ-domain-binding motif (Kibar et al., 2001; Murdoch et al., 2001). *Vangl2*$^{Lp/Lp}$ homozygous mutants display typical PCP phenotypes, including a shortened body axis, an open neural tube, and misorientation of sensory hair cells of the cochlea, whereas *Vangl2*$^{Lp/+}$ heterozygous mutant mice show a weak PCP-related phenotype, that is, a looped tail (Greene et al., 1998; Montcouquiol et al., 2003). Because mice with a heterozygous mutation of *Vangl2* display a weak PCP-related phenotype, additional introduction of a PCP mutation would exacerbate the mutant phenotype. The *Cthrc1*$^{LacZ/+}$;*Vangl2*$^{Lp/+}$ embryos were indistinguishable from those of *Vangl2*$^{Lp/+}$ mice (Figure 2B). By E13.5, *Cthrc1*$^{LacZ/LacZ}$;*Vangl2*$^{Lp/+}$ embryos displayed a neural tube closure defect in the midbrain region reminiscent of the PCP mutation (Figure 2C; Figure S1B available online). Although this defect was constantly observed in a mixed 129 SvEv/C57B6 background (n = 2/2 at E13.5, n = 2/2 at E18.5), it was not observed when mutants were further crossed with outbred (CD-1) mice (n = 6/6).

To confirm the genetic interactions of *Cthrc1* and *Vangl2*, we examined another characteristic feature of the PCP mutants—misorientation of the sensory hair cells in the cochlea. The normal cochlea has four rows of sensory hair cells—one row of inner hair cells (IHCs) and three of outer hair cells (OHCs). Each cell contains an asymmetrically located kinocilium at the outer side accompanied by a bundle of stereocilia. At E18.5, *Cthrc1*$^{LacZ/+}$;*Vangl2*$^{Lp/+}$ embryos showed a normal arrangement of four rows of hair cells and a uniform hair bundle orientation (Figures 2D–2G). In *Cthrc1*$^{LacZ/LacZ}$;*Vangl2*$^{Lp/+}$ embryos, however, the orientation of the hair bundles was disrupted significantly (Figures 2I–2K). Scanning electron microscopy confirmed the normal organization of ciliary bundles in the mutants, indicating that the defect was restricted to cell polarity (Figure 2I). Among the four rows of auditory hair cells, the IHCs were the most severely affected (Figure 2K). Severe defects were also present in the outermost row of OHCs (OHC3), and modest effects were observed in the inner rows (OHC1 and OHC2) (Figure 2K). This defect was not affected by the genetic background of the mutants (n = 8/8). In addition to the defects in the orientation of individual hair cells, we observed that some hair cells deviated from the rows, and, in an extreme case, additional sensory hair cells outside of the four rows were observed (Figure 2H, arrowheads). These results demonstrate the genetic interaction of *Cthrc1* with *Vangl2* for PCP signaling and suggest that *Cthrc1* is involved in the regulation of PCP signaling.

Interaction of Cthrc1 with Extracellular Components of Wnt/PCP Signaling

Involvement of *Cthrc1* in PCP signaling led us to investigate how *Cthrc1* controls PCP signaling. Because Cthrc1 is a secreted protein and because vertebrate PCP signaling is regulated by Wnt proteins, we examined the interaction of Cthrc1 with various extracellular components of Wnt signaling. For this purpose, we developed an interaction assay that immunoprecipitates the proteins from the lysates of cocultured HEK293T cells that were individually transfected with expression plasmids for Cthrc1 or various Wnt components (coculture IP). We used this method because the conditioned medium of Cthrc1-expressing cells had no activity (data not shown). We first verified the specificity of the protein interactions detected with this assay by using established interactions. Previous studies suggest the selective interaction of Wnt3a and Wnt5a with coreceptors: Wnt5a interacts with Ror2, but not with LRP5/6, and Wnt3a interacts with LRP5/6, but not with Ror2 (Liu et al., 2005; Mikels and Nusse, 2006; Oishi et al., 2003). In coculture IP, Wnt3a- or Wnt5a-expressing cells and Ror2- or LRP6-expressing cells were mixed and cocultured for 24 hr, and then Ror2 or LRP6 receptors were immunoprecipitated from the cell lysates (Figure 3A). Consistent with previous observations, Wnt3a was coprecipitated with LRP6, but not with Ror2, whereas Wnt5a was coprecipitated with Ror2, but not with LRP6 (Figure 3B, lanes 7, 8, 11, and 12). Both Wnt proteins failed to coprecipitate with EGFR or LDLR, negative controls for Ror2 or LRP6, respectively (Figure 3B, lanes 9, 10, 13, and 14). Therefore, coculture immunoprecipitation (IP) is a simple and reliable method by which to detect specific protein-protein interactions in the extracellular space.

Using coculture IP, we first examined the interaction of Cthrc1 with Fzd proteins. Cthrc1 was coprecipitated with Fzd3, Fzd5, and Fzd6, indicating interaction of Cthrc1 with multiple Fzd proteins (Figure 3C, lanes 6–8). No binding was observed between Cthrc1 and an Fzd-related protein, Smo, or a C-terminally truncated Cthrc1 (Cthrc1-ΔC) and Fzd6 (Figure 3C, lanes 9 and 10). We next examined the interaction of Cthrc1 with coreceptors Ror2 and LRP6. Cthrc1 was coprecipitated with Ror2 (Figure 3D, lane 8). The lack of interactions between Cthrc1 and EGFR and between Cthrc1-ΔC and Ror2 demonstrates the specificity of the Cthrc1-Ror2 interaction (Figure 3D, lanes 10 and 14). Cthrc1 also interacted with Ror2-ΔCRD, which lacks a cysteine-rich Wnt-interacting domain, indicating that Cthrc1 and Wnt interact with distinct domains of Ror2 (Figure 3D, lane 9). Cthrc1 was not coprecipitated with LRP6 or its negative control, LDLR (Figure 3D, lanes 11 and 12).

We next applied coculture IP to interactions between Cthrc1 and Wnt proteins. Although both Cthrc1 and Wnt proteins were supposed to be secreted, immunoprecipitation of Cthrc1 from the cell lysates coprecipitated both canonical Wnt (Wnt3a) and noncanonical Wnt proteins (Wnt5a and Wnt11) (Figure 3E, lanes 7, 10, and 13). Because Wnt proteins were not coprecipitated with Cthrc1-ΔC (Figure 3E, lanes 8, 11, and 14), the observed Cthrc1-Wnt interactions are specific. Finally, we also examined interaction of Cthrc1 with a transmembrane PCP signaling component, Vangl2. Although Cthrc1 and Vangl2 interacted genetically, these proteins did not interact physically (Figure 3D, lane 13). In summary, Cthrc1 interacts with multiple extracellular components of Wnt signaling, which include both canonical and noncanonical Wnt proteins, Fzd proteins, and the Wnt/PCP coreceptor Ror2, but not with the canonical Wnt coreceptor LRP6 or the PCP component Vangl2. These results suggest that Cthrc1 regulates PCP signaling by modulating Wnt signaling in the extracellular space.

Activation of the Wnt/PCP Pathway by Cthrc1

In vertebrates, the Wnt/PCP signal is transduced to two parallel signaling cascades, a process that starts with the activation of the small GTPases Rac1 and RhoA, downstream of dishevelled (Dvl) (Habas et al., 2003). To test whether Cthrc1 actually modulates the PCP pathway, we examined the effects of Cthrc1 on the

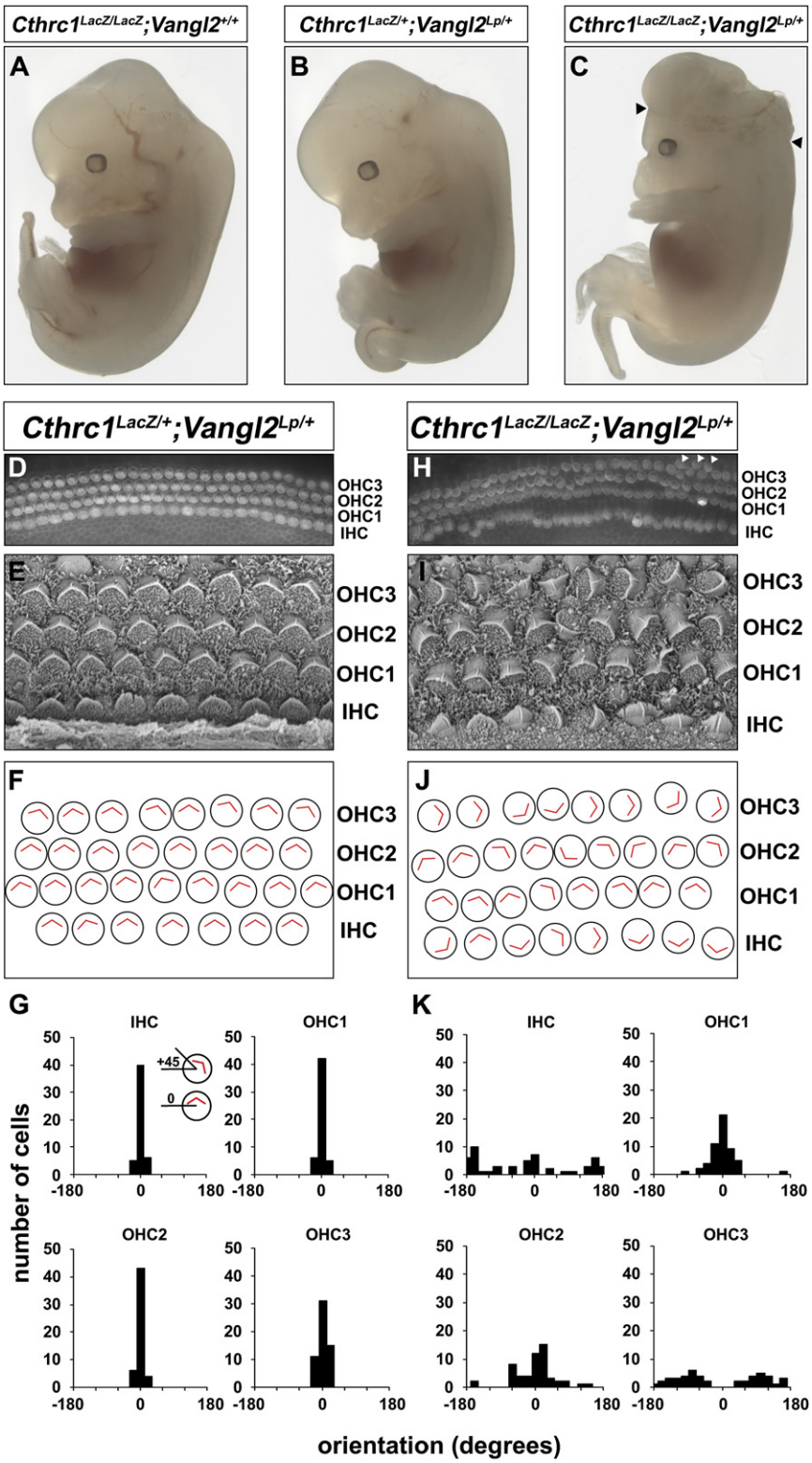

Figure 2. Genetic Interaction between *Cthrc1* and *Vangl2*

(A–C) Defects in anterior neural tube closure. At E13.5, (A) *Cthrc1*$^{LacZ/LacZ}$ embryos were normal, and (B) *Cthrc1*$^{LacZ/+}$;*Vangl2*$^{Lp/+}$ embryos showed only a curly tail phenotype, similar to the *Vangl2*$^{Lp/+}$ embryos. (C) *Cthrc1*$^{LacZ/LacZ}$;*Vangl2*$^{Lp/+}$ embryos displayed neural tube closure defects in the midbrain region.

(D–K) Defects in the orientation of ciliary bundles of sensory hair cells in the organ of Corti. (D and H) Falloidin staining and (E and I) scanning electron microscopy of the basal turn (25% from the basal end) of the organ of Corti. (F) and (J) are schematic representations of (E) and (I), respectively. (G) and (K) show the distribution of ciliary bundle orientation. A total of 54 cells were counted from 2 embryos for each genotype.

activities of Rac1 and RhoA in HEK293T cells, which have been successfully used for the analysis of Wnt/PCP signaling in mammals (Habas et al., 2001, 2003). This cell line expresses *Wnts*, *Ror2*, *LRP5/6*, and *Cthrc1* (Figure S2). To detect the activation of Rac1 and RhoA, we used an established biochemical assay that employs a fusion protein of glutathione S-transferase and the p21-binding domain of human PAK-1 (GST-PBD) and GST-RBD (Rho-binding domain of mouse rhotekin fused with GST) that recognizes GTP-bound forms (i.e., active forms) of Rac and Rho, respectively. Transfection of the expression plasmids for *Wnt3a*, *Wnt5a*, or *Dvl2* activated endogenous Rac1 (Figure 4A, lanes 3, 5, and 7), and a similar activation was also observed by transfection of the *Cthrc1* expression plasmid (Figure 4A, lane 2). Coexpression of Cthrc1 with Wnt3a, Wnt5a, or Dvl2 further enhanced the activation of Rac1 (Figure 4A, lanes 4, 6, and 8). Similarly, Cthrc1 also activated RhoA (Figure 4B, lane 2) and enhanced activation of RhoA by Wnt3a, Wnt5a, or Dvl2 (Figure 4B, lanes 3–8). These results suggest that Cthrc1 activates both cascades of the Wnt/PCP pathway, and this effect is synergistic with pathway activation by other signaling components.

Non-Cell-Autonomous Suppression of Canonical Wnt Signaling by Cthrc1

We next investigated whether Cthrc1 also modulates canonical Wnt signaling. To monitor the activation of the canonical Wnt pathway, we used the Wnt reporter TOPFLASH, which expresses the luciferase gene under the control of TCF-binding sites. Although expression of Cthrc1 by itself had no effect on the expression of the reporter, when the reporter was activated by cotransfection of *Wnt3a* and *LRP6* plasmids, Cthrc1 repressed this activation in a dose-dependent manner (Figure 4C).

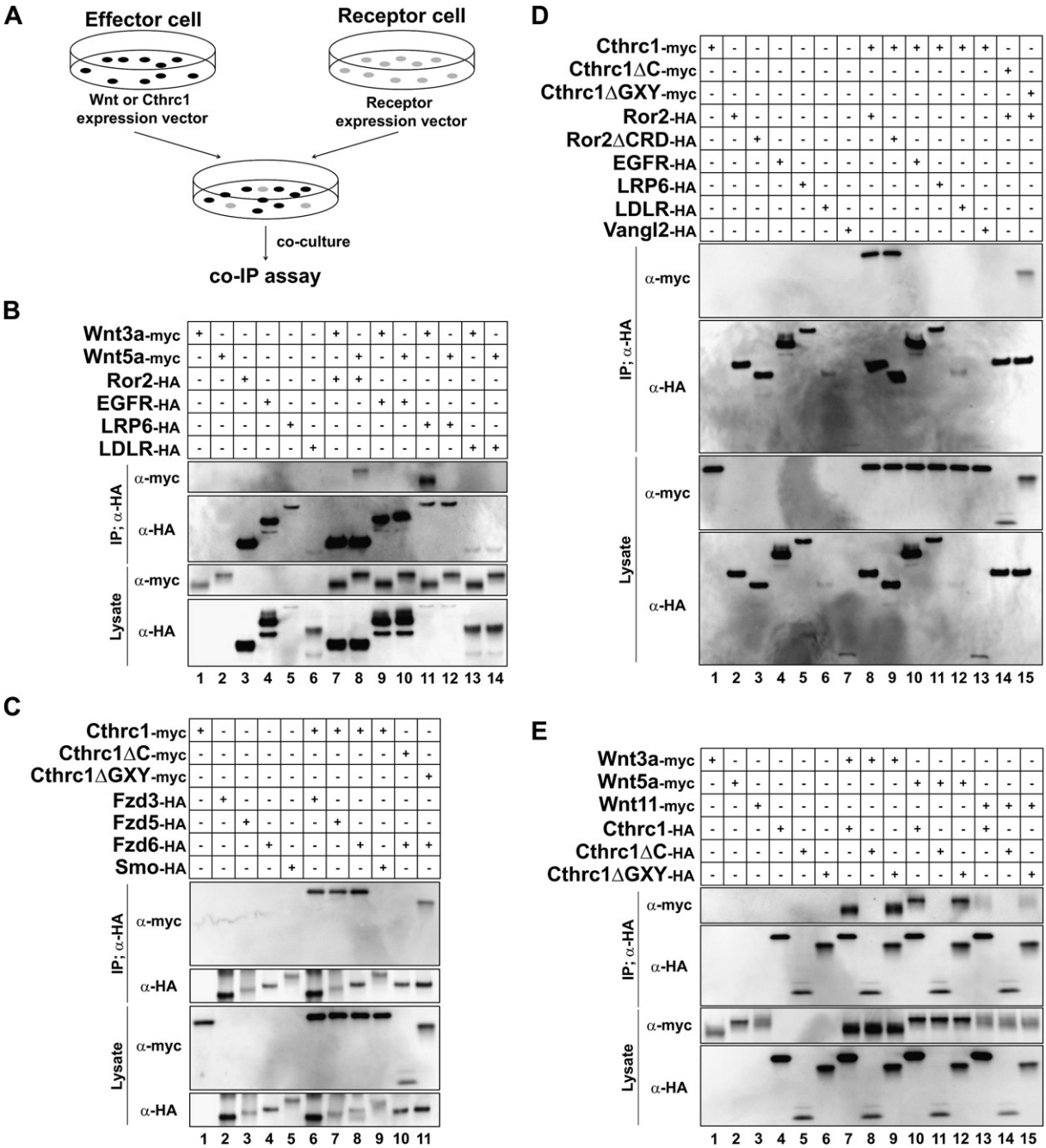

Figure 3. Interaction of Cthrc1 and Wnt Signaling Components

(A) Scheme of the coculture IP procedure.

(B) Coculture IP detected the specific interaction between Wnt3a/5a and coreceptor Ror2 or LRP6.

(C) Interaction of Cthrc1 with Fzd receptors.

(D) Interaction of Cthrc1 with coreceptors.

(E) Interaction of Cthrc1 with Wnt proteins.

Interestingly, Cthrc1 also suppressed the Wnt reporter stimulated by an intracellular signaling component, Dvl2, but not by β-catenin, a component further downstream (Figure 4C).

Intracellular inhibition of the canonical pathway raised the possibility that overexpressed Cthrc1 acted in the intracellular space, which could be a nonphysiological function. To exclude this possibility, the non-cell-autonomous activity of canonical pathway suppression by Cthrc1 was examined by conducting coculture experiments. We first prepared effector cells transfected with expression plasmids for *Wnt3a*, *Cthrc1*, or an empty plasmid and reporter cells transfected with the TOPFLASH reporter. Then, the effector and reporter cells were cocultured for

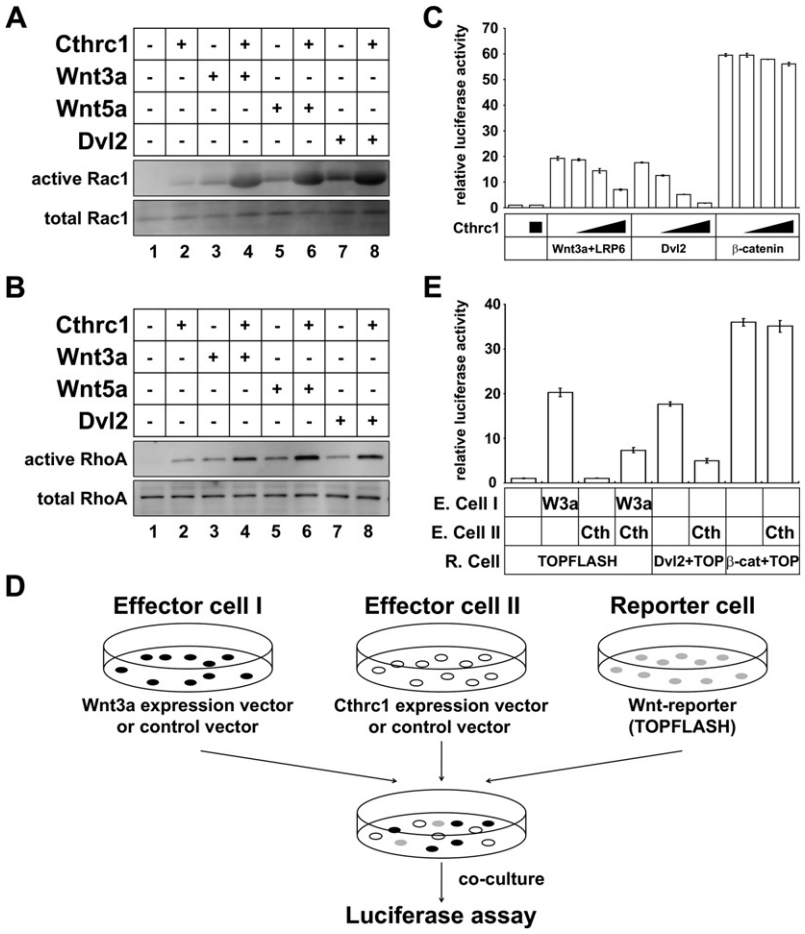

Figure 4. Effect of Cthrc1 on Wnt/PCP and Canonical Wnt Signaling

(A and B) Activation of the Wnt/PCP pathway by Cthrc1. Cthrc1 weakly activated downstream components of the PCP pathway: (A) Rac1 and (B) RhoA. Cthrc1 also enhanced activation of Rac1 and RhoA by Wnt3a, Wnt5a, or Dvl2.

(C) Suppression of the canonical Wnt pathway by Cthrc1. The graphs show the average of two samples with standard errors.

(D) Scheme of the coculture experiment.

(E) Non-cell-autonomous effect of Cthrc1. Cthrc1 suppressed activation of the canonical pathway in a non-cell-autonomous manner. The graphs show the average of two samples with standard errors.

24 hr before measurement of luciferase activity (Figure 4D). Wnt3a cells efficiently activated TOPFLASH, and this activation was clearly suppressed by the presence of Cthrc1 cells (Figure 4E). Furthermore, activation of TOPFLASH by Dvl2 in the reporter cells was also suppressed by the presence of Cthrc1 cells (Figure 4E). Suppression was not observed when the reporter was activated by β-catenin. These results suggest that Cthrc1 acts in a non-cell-autonomous manner and suppresses the canonical pathway. Furthermore, extracellular Cthrc1 also suppresses the canonical pathway activated by Dvl, although the underlying mechanism is currently unknown (see the Discussion).

Identification of the Functional Domain of Cthrc1

Because Cthrc1 contains characteristic GXY repeats and an evolutionally conserved C-terminal region, we studied domains responsible for the activities of Cthrc1 by using the deletion constructs (Figure 5A). Cthrc1 and the GXY-repeat deletion mutant (ΔGXY) bound to Wnt3a, Wnt5a, and Wnt11, unlike the C-terminal deletion mutant (ΔC) (Figure 3E, lanes 7–15). Activation of the Wnt/PCP pathway revealed by activation of Rac1 and RhoA was also observed with ΔGXY, but not with ΔC (Figures 5B and 5C, lanes 3 and 4). Similar to full-length Cthrc1, we also observed a synergistic effect of ΔGXY and Wnt5a on the activation of Rac1 and RhoA, whereas ΔC had no effect on activation of Rac1 and RhoA by Wnt5a (Figures 5B and 5C, lanes 5–8). ΔGXY also suppressed Wnt reporter activity stimulated by Wnt3a and LRP6 as effectively as full-length Cthrc1, unlike ΔC (Figure 5D). Therefore, the C-terminal region is responsible for all of the known activities of Cthrc1, and the GXY repeat is dispensable.

Cthrc1 is an *N*-glycosylated protein, and treatment of Cthrc1 in the conditioned medium (CM) with *N*-glycosidase F removed *N*-glycosylation and resulted in faster migration in SDS-polyacrylamide gel electrophoresis (PAGE), as reported previously (Pyagay et al., 2005; Figure 5E, lanes 1 and 2). The C-terminal region of Cthrc1 contains a putative *N*-glycosylation site. Sequence alteration of this motif (N188A; replacement of asparagine at position 188 by alanine) resulted in faster electrophoretic mobility, and this mobility was not altered by *N*-glycosidase F treatment (Figures 5A and 5E, lanes 5 and 6), indicating the absence of *N*-glycosylation in N188A. Because N188A bound to Wnt5a and suppressed canonical Wnt signaling (Figures 5F and 5G), *N*-glycosylation of Cthrc1 is dispensable for the Wnt/PCP regulatory activity of Cthrc1.

Identification of the Active Form of Cthrc1

Coculture of Cthrc1-expressing cells suppressed canonical Wnt signaling, unlike its conditioned medium (data not shown). To reveal the cause of such differences, we compared Cthrc1 proteins in the cell lysate (Cthrc1-L) and in the conditioned medium (Cthrc1-CM). Cthrc1-CM showed slower migration than Cthrc1-L on SDS-PAGE (Figure 5E, lanes 1 and 3), indicating that only the modified protein is released into the medium. Treatment of Cthrc1-L with *N*-glycosidase F resulted in faster mobility identical to that of N188A (Figure 5E, lanes 3 and 4), suggesting that Cthrc1-L is *N*-glycosylated and that Cthrc1-CM has an additional modification that is not *N*-glycosylation. Although the identity of this additional modification of Cthrc1-CM is not known, the modification appeared to depend on *N*-glycosylation, because N118A did not produce modified protein in the conditioned medium (Figure 5E, lane 5). Because N188A was reproducibly detected in conditioned medium, although the amount was much lower than in Cthrc1-CM (note that ten times more conditioned

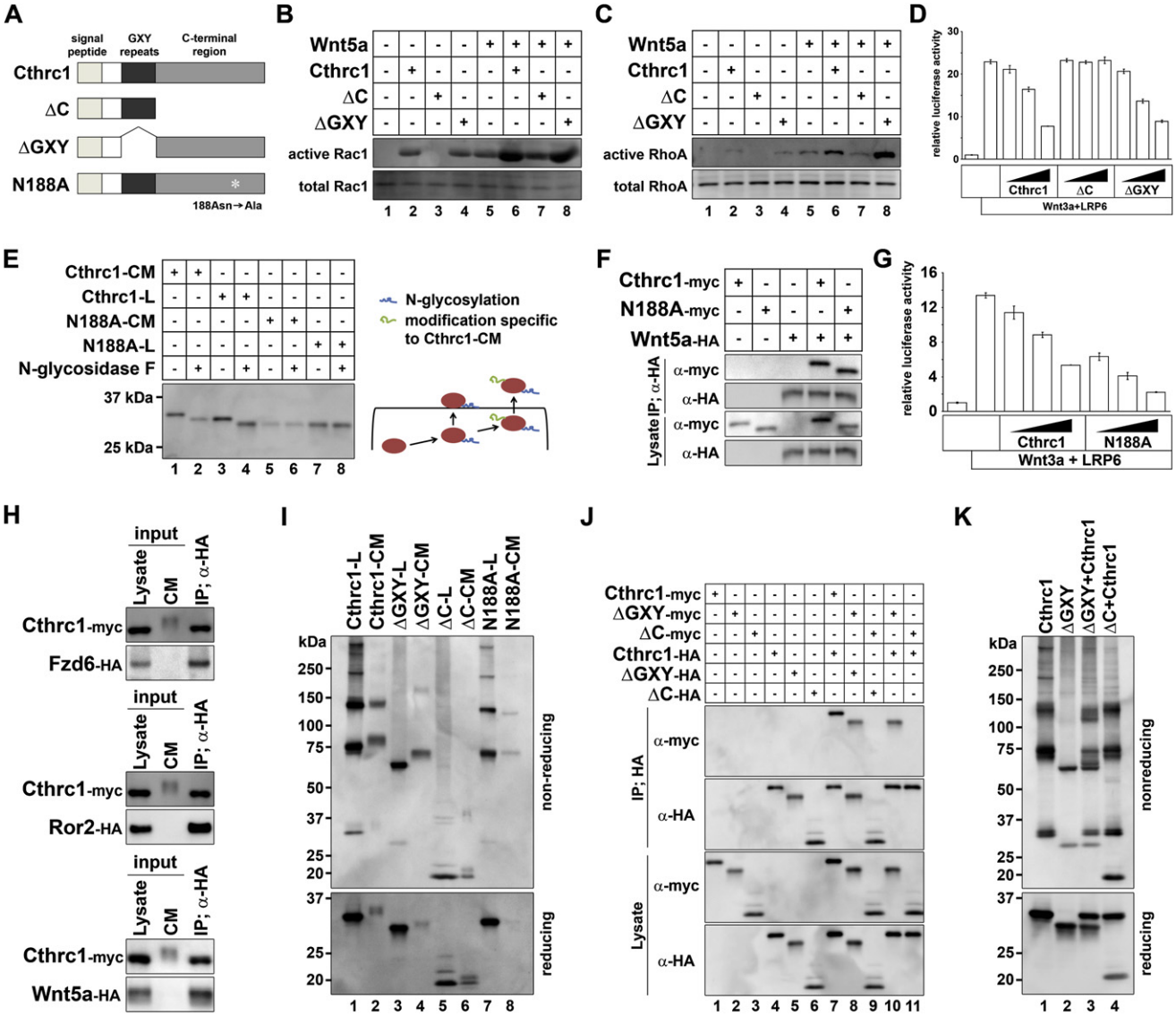

Figure 5. Identification of the Active Form of Cthrc1

(A) Cthrc1 mutants used in this study.

(B–D) Effects of domain deletions on the activation of PCP pathway components, (B) Rac1 and (C) RhoA, and on the (D) suppression of the canonical pathway. The graphs show the average of two samples with standard errors.

(E–G) Presence of two modifications in Cthrc1. N188A (E) lacks *N*-glycosylation, (F) binds to Wnt5a, and (G) suppresses canonical Wnt signaling. The graphs show the average of two samples with standard errors.

(H) Interaction of Wnt signaling components with Cthrc1-L, but not with Cthrc1-CM.

(I–K) Cthrc1 forms a multimer, as revealed by higher molecular weight on (I) nonreducing SDS-PAGE, (J) immunoprecipitation, and (K) coexpression of full-length Cthrc1 and ΔGXY.

medium was used for N188A-CM in Figure 5E), *N*-glycosylation may contribute to the anchorage of Cthrc1 on the cell surface, and additional modification specific to Cthrc1-CM may release it. In a coculture IP, immunoprecipitation of Fzd6, Ror2, or Wnt5a coprecipitated Cthrc1-L from the lysate, but not Cthrc1-CM, although Cthrc1-CM was also present during the coculture period (Figure 5H). These results suggest that Cthrc1-L anchored on the cell surface is an active protein, whereas Cthrc1-CM has no activity because it lacks binding activity to the Wnt/PCP components.

When Cthrc1-L and Cthrc1-CM were electrophoresed by using a nonreducing SDS-PAGE, both proteins produced multiple bands (Figure 5I, lanes 1 and 2). In addition to the 75 kDa band, which was previously characterized as a trimer of Cthrc1 peptides (Pyagay et al., 2005), we observed strong bands at 150 kDa, 250 kDa, and a higher molecular mass. ΔGXY produced a major band at 70 kDa. Although the GXY repeat resembles the multimerization domain of collagens, this size of ΔGXY is much larger than the size of the monomer and is close to the size of the Cthrc1 trimer. Therefore, ΔGXY may also form a trimer.

This hypothesis is supported by the observation that, when HA-tagged and myc-tagged ΔGXY were coexpressed, immunoprecipitation of HA-tagged ΔGXY coprecipitated myc-tagged ΔGXY (Figure 5J, lane 8). Furthermore, coexpression of ΔGXY and full-length Cthrc1 produced multiple bands around 70–75 kDa (Figure 5K, lane 3). A similar intermolecular interaction was also observed with proteins containing the C-terminal region, but not with ΔC (Figure 5J, lanes 7–11, and Figure 5K, lane 4). Because ΔGXY did not produce multiple bands at a higher molecular mass (Figure 5I, lanes 3 and 4), the GXY repeat is likely to be involved in the generation of a higher-order multimer, i.e., a multimer of the Cthrc1 trimer. Taking these results with those of the functional analyses described above, the normal active form of Cthrc1 should be an *N*-glycosylated trimer anchored on the cell surface.

Enhancement of the Ligand-Receptor Interaction for the Wnt/PCP Pathway by Cthrc1

The selective activation of the PCP pathway by Cthrc1 led us to examine its underlying mechanisms. Because Cthrc1 interacted with Wnt and receptors, Cthrc1 may modulate the ligand-receptor interaction. We tested this hypothesis in coculture IP by precipitating the receptors from lysates of cocultured cells, which individually express Wnt, Cthrc1, or receptors, followed by determination of the amount of coprecipitated Wnt proteins by western blot. We first examined whether interaction of Wnt and Fzd proteins is influenced by Cthrc1. We used Wnt3a and Wnt5a as representative canonical and noncanonical Wnt proteins, respectively. As shown in Figure 6A, Cthrc1 and Wnt3a were coprecipitated with Fzd5, and Cthrc1 enhanced binding of Wnt3a and Fzd5, as revealed by the stronger band of precipitated Wnt3a (lanes 6 and 7). Relative amounts of the precipitated Wnt proteins were quantified and are represented as shown in Figure 6A′. Similar enhancement of the Wnt-Fzd interaction by Cthrc1 was also observed for all of the combinations of Wnt3a/Wnt5a and Fzd5/Fzd6 (Figures 6A and 6A′, lanes 6–13). The absence of the enhancement of the Wnt-Fz interaction by Cthrc1-ΔC (Figures S3A and S3A′) and the absence of an interaction between Cthrc1-Wnt and Smo (Figure 6A, lanes 14 and 15) confirmed the specificity of this effect. Therefore, Cthrc1 forms a ternary complex of Cthrc1-Wnt-Fzd and enhances the interaction between Wnt proteins and Fzd proteins. There is no clear preference in this enhancement based on the classes of Wnt proteins.

We next examined the effect of Cthrc1 on the interaction between Wnt proteins and the pathway-specific coreceptors Ror2 (PCP pathway) and LRP6 (canonical pathway). As shown in Figures 6B and 6B′, Wnt3a was not significantly coprecipitated with Ror2; however, in the presence of Cthrc1, Wnt3a was clearly coprecipitated with Ror2 (lanes 6 and 7). Cthrc1 did not affect the interaction of Wnt3a and LRP6 (lanes 8 and 9). Wnt5a was coprecipitated with Ror2, and, in the presence of Cthrc1, this interaction was enhanced, as revealed by stronger bands (lanes 10 and 11). Wnt5a was not coprecipitated with LRP6, and Cthrc1 did not affect the binding of Wnt5a and LRP6 (lanes 12 and 13). Confirming the specificity of the observed interactions, Cthrc1-ΔC had no effect on the interaction of Wnt3a/5a and Ror2 (Figures S3B and S3B′), and no binding of Cthrc1-Wnt and EGFR was observed (Figure 6B, lanes 14 and 15). Therefore, regardless of the Wnt class, Cthrc1 selectively enhanced the interaction between Wnt and Ror2 by forming the ternary complex Cthrc1-Wnt-Ror2.

Although Cthrc1 generally enhanced the Wnt-Fzd interaction, it selectively enhanced the Wnt-coreceptor interaction. Because both Fzd and coreceptors may be present in the normal situation, we next examined whether selective enhancement of the Wnt-(co)receptor interaction was also observed under such conditions. In these experiments, Fzd and coreceptor were expressed in the same cells. As shown in Figures 6C and 6C′, Cthrc1, Wnt3a, and Ror2 or LRP6 were coprecipitated with Fzd6, and Cthrc1 enhanced the Wnt3a-Fzd6 interaction in the presence of Ror2 (lanes 7 and 8), but not in the presence of LRP6 (lanes 9 and 10). Similarly, Ror2-specific enhancement of the Wnt5a-Fzd6 interaction by Cthrc1 was also observed (lanes 11–14). No enhancement was observed with Cthrc1-ΔC (Figures S3C and S3C′). Immunoprecipitation of Ror2 or LRP6 from the lysates further confirmed the selective enhancement of the Wnt3a/5a-Fzd6-Ror2 interaction by Cthrc1, and no enhancement of the Wnt3a/5a-Fzd6-LRP6 interaction (Figures 6D and 6D′). Again, no enhancement was observed with Cthrc1-ΔC (Figures S3D and S3D′). Essentially, the same results were obtained with Fzd5, indicating that the effect of Cthrc1 is not specific to Fzd6 (data not shown). Therefore, in the presence of both Fzd and coreceptors, general enhancement of binding of Wnt and Fzd by Cthrc1 was not observed. Instead, Cthrc1 selectively enhanced the interaction of Wnt with receptors for the PCP pathway, Fzd and Ror2, by forming the complex of Cthrc1-Wnt-Fzd, Cthrc1-Wnt-Ror2, or Cthrc1-Wnt-Fzd-Ror2. These three complexes are hereafter collectively referred to as Cthrc1-Wnt-Fzd/Ror2. Such pathway-specific enhancement of the ligand-receptor interaction is likely to be a molecular basis for the selective activation of the Wnt/PCP pathway by Cthrc1.

Misorientation of the Cochlear Sensory Hair Cells in *Ror2*$^{-/-}$ Mice

The interaction analyses suggest that Ror2 plays a key role in the selective activation of Wnt/PCP signaling by Cthrc1. Although Ror2 has been characterized as a Wnt receptor activating Wnt/PCP signaling in cell culture and frog embryos (Hikasa et al., 2002; Oishi et al., 2003), the relationship between abnormalities reported with *Ror2*$^{-/-}$ mutant mice (e.g., short limbs and tails) (DeChiara et al., 2000; Takeuchi et al., 2000), and PCP signaling is currently unclear. If Cthrc1 functions by forming the Cthrc1-Wnt-Fzd/Ror2 complex, *Ror2*$^{-/-}$ mutants should also exhibit PCP-related inner ear defects similar to those of *Cthrc1*$^{LacZ/LacZ}$; *Vangl2*$^{Lp/+}$ embryos. Whole-mount in situ hybridization revealed widespread expression of *Ror2* in E18.5 cochlea, but the strong signal was restricted to the sensory hair cells of the organ of Corti (Figure 7A, left), which also express *Cthrc1* (Figure 1H). No signal was observed with a sense probe (Figure 7A, right). At E18.5, all of the *Ror2*$^{-/-}$ embryos showed disruption in organization of the organ of Corti (n = 5/5). Two of them showed strong randomization of orientation of auditory hair cells as well as disturbance of the alignment of OHCs into three rows with a local increase or decrease in the number of rows of OHCs (Figures 7D, 7E, and 7I, and data not shown). In the other three, abnormalities in the alignment of OHCs into three rows were evident, and the disruption of cell orientation was weak (Figures 7F, 7G, and 7J). Although the latter phenotype has not

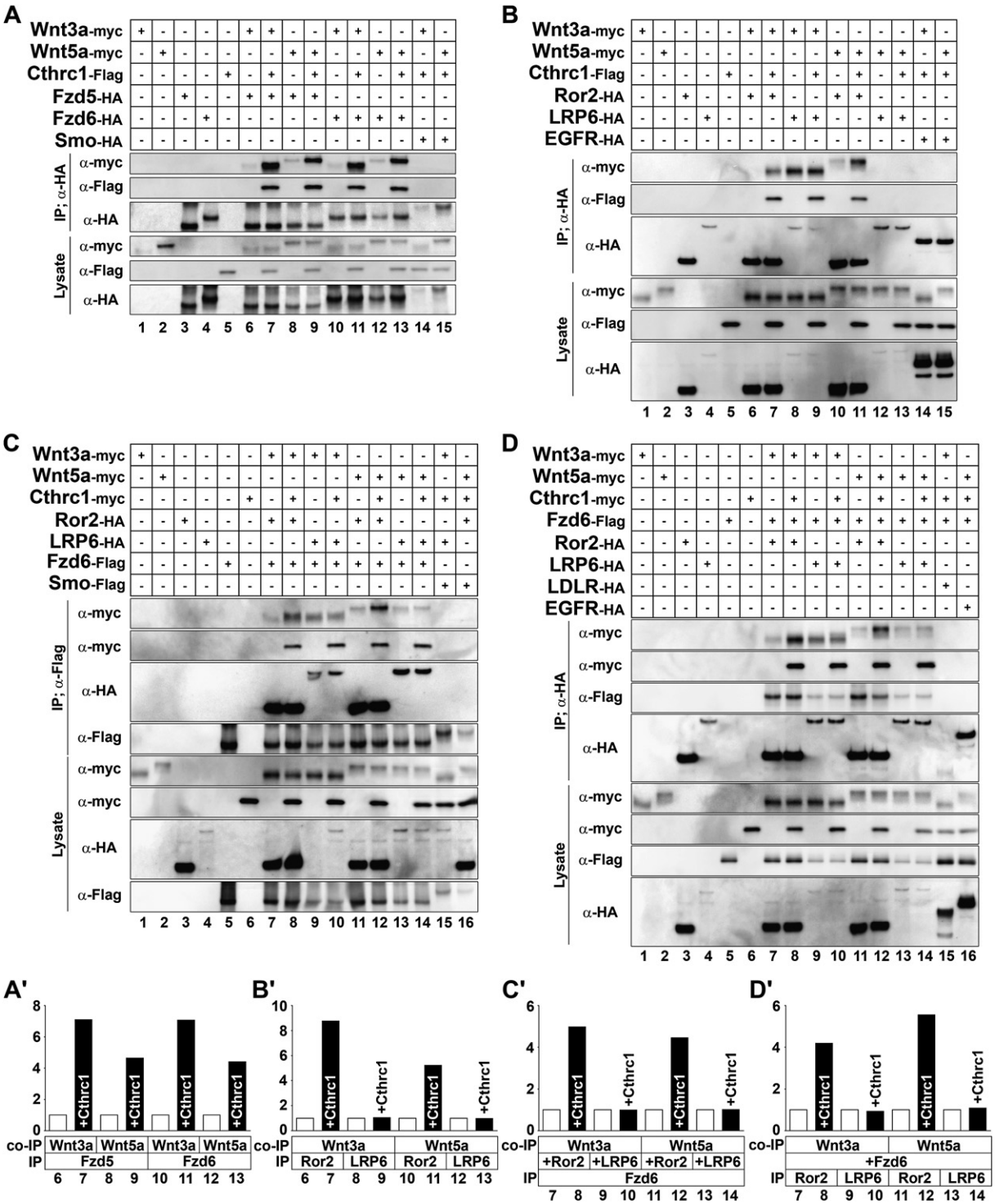

Figure 6. Effects of Cthrc1 on the Wnt-Receptor Interaction

(A–D) (A) Effects of Cthrc1 on the Wnt-Fzd interaction. (B) Effects of Cthrc1 on the Wnt-coreceptor interaction. (C and D) Effects of Cthrc1 on the Wnt-Fzd-coreceptor interaction. (A and C) Fzd or (B and D) coreceptors were immunoprecipitated from the cocultured lysates.

(A′–D′) Graphs representing the relative amounts of precipitated Wnt proteins in the experiments shown in (A)–(D), respectively. Lane numbers correspond to those in (A)–(D). Values are normalized to intensities without Cthrc1 as 1.

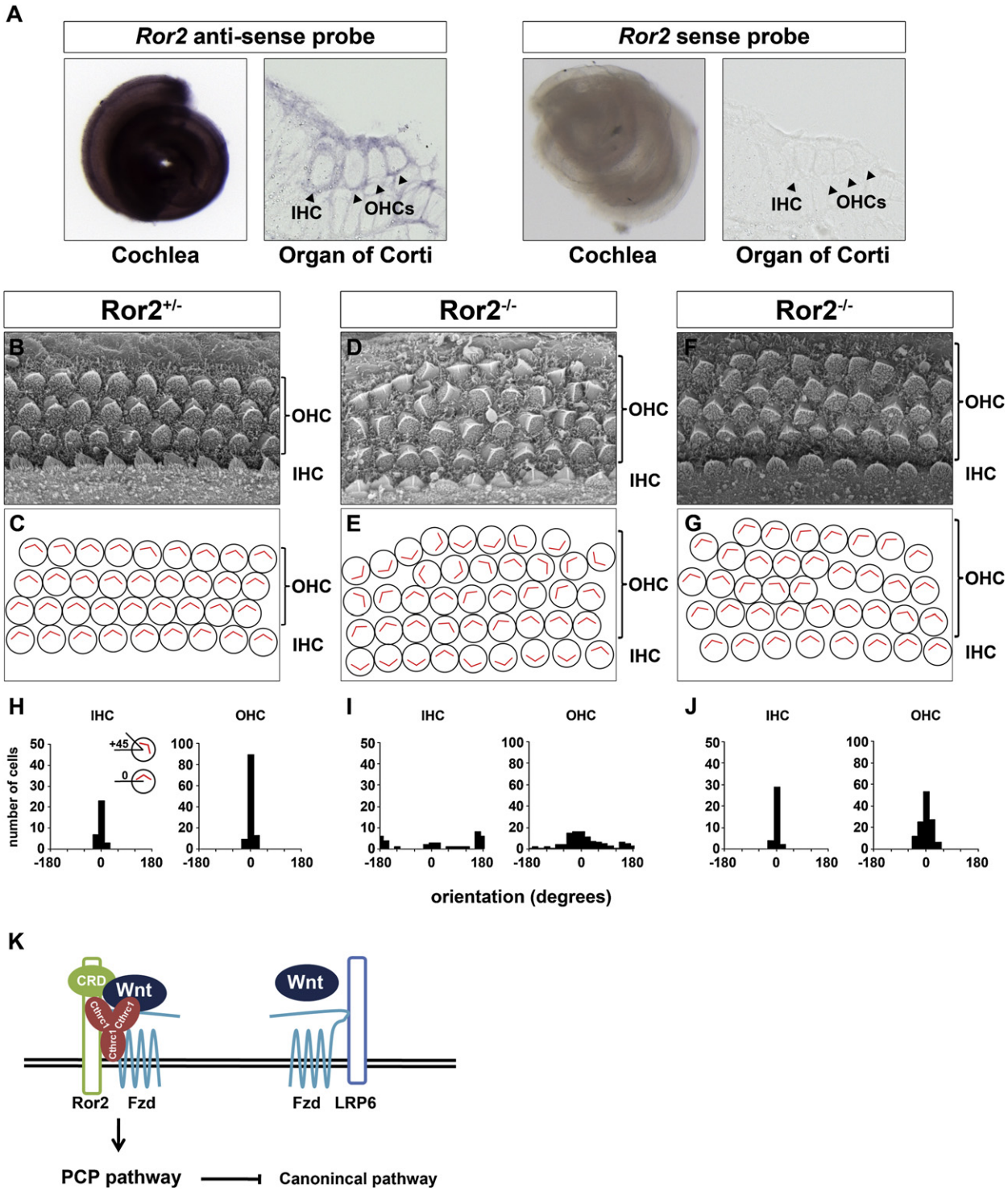

Figure 7. Involvement of *Ror2* in PCP Signaling in Inner Ear Development

(A) Expression of Ror2 mRNA in the inner ear.

(B–J) Defects of alignment and orientation of sensory hair cells. (B, D, and F) Scanning electron microscopy of the basal turn of the organ of Corti of (B) control and (D and F) *Ror2* homozygous mutant embryos. (C), (E), and (G) are schematic representations of (B), (D), and (F), respectively. (H)–(J) show the distribution of ciliary bundle orientation. Data in (H) were from two control embryos, and data in (I) and (J) were from the embryos shown in (D) and (J), respectively.

(K) Model of selective activation of the Wnt/PCP pathway by Cthrc1.

been reported with PCP mutant mice, the former phenotype is a representative abnormality observed with PCP mutants. Therefore, these results suggest that Ror2 regulates PCP signaling in inner ear development and supports the hypothesis that Cthrc1 forms a Cthrc1-Wnt-Fzd/Ror2 complex to activate PCP signaling in this tissue.

DISCUSSION

Previous studies revealed several mechanisms for pathway selection by Wnt proteins, which include intrinsic differences of Wnt and Fzd proteins and the availability of coreceptor proteins Ror2 and LRP5/6. We identified Cthrc1 as an extracellular component of the Wnt pathway that contributes to selective activation of the PCP pathway. This finding suggests the existence of a regulatory mechanism for pathway selection by Wnt proteins, which we would like to summarize in the following model (Figure 7K). There are some intrinsic preferences for interactions among Wnt, Fzd, and coreceptor proteins (Liu et al., 2005; Mikels and Nusse, 2006; Takada et al., 2005). However, in the conditions in which appropriate receptors are available, these Wnt proteins may form both Wnt-Fzd-LRP5/6 and Wnt-Fzd/Ror2 complexes and activate the canonical Wnt and Wnt/PCP pathways. The interaction of Wnt proteins with Fzd/Ror2 is selectively enhanced in the presence of Cthrc1 by forming the Cthrc1-Wnt-Fzd/Ror2 complex. Although Wnt-Fzd and Wnt-Ror2 have been implicated in noncanonical Wnt signaling, whether Fzd and Ror2 act within a single receptor complex, or whether they act in two parallel pathways, is currently not known. Our results did not resolve this issue, and, therefore, the Cthrc1-Wnt-Fzd/Ror2 complex could be Cthrc1-Wnt-Fzd, Cthrc1-Wnt-Ror2, or Cthrc1-Wnt-Fzd-Ror2. However, we prefer the model of Cthrc1-Wnt-Fzd-Ror2 complex formation, because it is known that Ror2 interacts with several Fzd proteins (Oishi et al., 2003), and because the cell migratory activity of Wnt5a/Ror2 signaling requires Dvl, a downstream effector of Fzd signaling (Nishita et al., 2006). The effect of Cthrc1 is not restricted to the enhancement of preexisting interactions, such as that of Wnt5a with Ror2, and it also establishes new interactions, such as that of Wnt3a with Ror2. The normal active form of Cthrc1 is an *N*-glycosylated trimer anchored on the cell surface. Because Cthrc1 interacts with Wnt proteins, Fzd proteins, and Ror2, Cthrc1 may bridge these proteins through trimer formation. Cthrc1 does not bind to LRP5/6, and the interaction of Wnt with Fzd-LRP5/6 is not affected by Cthrc1. The selective enhancement of Wnt-receptor binding results in the selective activation of the Wnt/PCP pathway and suppression of the canonical pathway. Suppression of the canonical pathway should be a secondary effect as a result of strong activation of the PCP pathway, because interaction of Wnt and Fzd-LRP6 was not affected by Cthrc1, and because activation of PCP signaling with intracellular components suppresses the canonical Wnt pathway (Park and Moon, 2002; Veeman et al., 2003b). Expression of multiple *Wnt* genes in HEK293T cells obscured whether Cthrc1 by itself is sufficient for activation of the PCP pathway or whether Wnt proteins are required. Although we could not rule out the former possibility, the formation of a Cthrc1-Wnt-Fzd/Ror2 complex supports the latter mechanism.

In vivo, the model of PCP activation by the Cthrc1-Wnt-Fzd/Ror2 complex is best supported by inner ear development. The cochlea undergoes a morphogenetic movement known as "convergent extension" to elongate and properly align the sensory hair cells of the organ of Corti (Qian et al., 2007). Such morphogenesis is disrupted in mouse mutants of PCP signaling components (*Vangl2*, *Celsr1*) (Montcouquiol et al., 2003; Wang et al., 2005), and similar defects are also observed with the mouse mutants *Cthrc1*$^{LacZ/LacZ}$;*Vangl2*$^{Lp/+}$, *Wnt5a*$^{-/-}$, *Fzd3*$^{-/-}$; *Fzd6*$^{-/-}$, and *Ror2*$^{-/-}$, which was consistent with our study (Qian et al., 2007; Wang et al., 2006b). Therefore, it is conceivable that the Cthrc1-Wnt5a-Fzd3/Fzd6/Ror2 complex activates PCP signaling in this tissue. Although *Wnt7a* is also expressed in the cochlea (Dabdoub et al., 2003), no activation of canonical Wnt signaling is observed (Qian et al., 2007). Therefore, Cthrc1 may also support cochlea development by assuring the selective activation of the PCP pathway by Wnt proteins. Although overexpression of Cthrc1 clearly suppresses the canonical Wnt pathway, to determine whether endogenous levels of Cthrc1 are sufficient for this activity requires further research. A similar mechanism may also take place in the notochord, which strongly expresses Cthrc1, because the notochord also undergoes convergent extension regulated by PCP signaling (Wang et al., 2006a; Ybot-Gonzalez et al., 2007), and canonical Wnt signaling should be suppressed in notochord development.

Cthrc1 promotes cell migration by reducing the deposition of the collagen matrix (Pyagay et al., 2005). We speculate that Wnt/PCP pathway activation by Cthrc1 also contributes to the promotion of cell motility. Because the PCP pathway regulates actin polymerization through activation of the small GTPases, JNK, and ROCK, activation of the PCP pathway should alter cellular morphology and increase cellular motility. During cancer development (Katoh and Katoh, 2007) and wound healing (Labus et al., 1998), activation of canonical Wnt signaling by transcriptional activation of canonical Wnt proteins and/or epigenetic silencing of secreted Wnt antagonists is observed. Therefore, additional expression of Cthrc1 to these cells (Pyagay et al., 2005; Tang et al., 2006) likely results in the activation of the PCP pathway and promotion of cellular motility. Consistent with this notion, Wnt/PCP signaling-related genes are overexpressed in some malignant (i.e., invasive and/or metastatic) human cancers (Katoh, 2005). Therefore, it is conceivable that Cthrc1 is a multifunctional protein and promotes cell migration through activation of Wnt/PCP signaling and reduction in collagen matrix deposition. Multifunctionality of Cthrc1 is also reported for TGF-β signaling. Cthrc1 in the conditioned medium, which has a specific modification and lacks Wnt modulating activity (this study), inhibits TGF-β signaling (LeClair et al., 2007), suggesting that modifications control the activity and localization of Cthrc1.

In conclusion, we identified a Wnt cofactor protein, Cthrc1, that promotes selective activation of the PCP pathway by enhancing the Wnt-receptor interaction. Identification of Cthrc1 suggests a mechanism for pathway selection by the Wnt proteins. This mechanism may be used widely in the regulation of morphogenesis during development and cell motility in wound healing and cancer metastasis. In an evolutionary context, it is of interest to note that Cthrc1 is present only in chordates (Pyagay et al., 2005), which use Wnt proteins for PCP signaling (Jones and Chen, 2007). The absence of apparent abnormality

in *Cthrc1* mutant mice suggests the presence of functionally redundant genes. The absence of *Cthrc1*-related genes in the mouse genome suggests that structurally distinct genes compensate for the absence of Cthrc1. Identification of such genes in the future should facilitate understanding of the mechanism of pathway selection by Wnt proteins.

EXPERIMENTAL PROCEDURES

Construction of a Single-Cell Notochord Library and In Situ Hybridization Screening

Transgenic mouse embryos expressing enhanced green fluorescent proteins (EGFPs) in the node and the notochord were obtained by crossing the two transgenic lines, CAG-CAT-EGFP (Kawamoto et al., 2000) and Not-Cre, which express Cre recombinase in the notochord (unpublished data). After the dissociation of E8.25 transgenic embryos by trypsin treatment, EGFP-positive node or notochord cells were manually picked up with a glass capillary under a fluorescence microscope. cDNAs from single node/notochord cells were synthesized and amplified as described previously (Yabuta et al., 2006). The resulting cDNA pools were analyzed individually for the appropriate gene expression profiles by virtual northern blot with *Foxa2*, *brachyury*, *Shh*, *Sox17*, *Mox1*, *Twist*, and *Ncam1* probes. The efficiency of cDNA amplification was assessed by using a G6PDH probe. A single-cell cDNA pool that showed clear expression of *Foxa2*, *brachyury*, and *Shh*, but not other genes, was selected for construction of a cDNA library in pBluescript II SK(−) (Stratagene). A total of 5292 clones were spotted on a nylon membrane in a 384-well format and were hybridized with total E9.5 cDNA probes. Abundantly expressed genes, which showed clear signals, were removed, and the remaining 2264 clones were sequenced and clustered. A total of 524 clones were analyzed for gene expression pattern by whole-mount in situ hybridization in 96-well plates as described previously (Neidhardt et al., 2000). This screening identified several genes expressed in the node and/or the notochord, including *Cthrc1*.

Generation of *Cthrc1* Mutant Mice

Cthrc1 mutant mice (CDB0502K) were generated as follows. A targeting vector was constructed by inserting a cassette consisting of *LacZ*-pA and *PGK-neo*-pA into the first exon of *Cthrc1* to replace the coding sequence with *LacZ* (Figure 1I). EB3 ES cells (Niwa et al., 2002) were electroporated with a linearized targeting vector and selected by G418, blasticidin S, and diphtheria toxin A fragment. ES cells carrying a recombinant allele were injected into eight-cell embryos of C57BL/6 mice to generate chimeric mice. Chimeric founders from two independent ES cell lines were crossed with C57BL/6 mice, and the resulting mutant mouse line was maintained on a C57BL/6 or CD1 background. Mice were housed in environmentally controlled rooms of the Laboratory Animal Housing Facility of the RIKEN Center for Developmental Biology, under the institutional guidelines for animal and recombinant DNA experiments. Other mouse strains and procedures for genotype determination are described in the Supplemental Data.

Analysis of the Organ of Corti

Temporal bones were dissected from mutant embryos at E18.5. The surrounding cartilage was removed to expose the cochlea, and the anlage of Reissner's membrane was dissected to expose the sensory epithelium. Dissected tissues were fixed in 4% paraformaldehyde at room temperature for 1 hr. To visualize the orientations of the stereociliary bundle, fixed tissues were stained with Alexa 568 phalloidin (Molecular Probes), as previously described (Wang et al., 2006b). Confocal images were obtained with an LSM510 META laser scanning microscope (Zeiss). For scanning electron microscopy, tissues were fixed with 2% fresh formaldehyde and 2.5% glutaraldehyde in 0.1 M sodium cacodylate buffer (pH 7.4) for 2 hr, followed by postfixation with 1% OsO_4 in the same buffer for 2 hr on ice. Samples were then dehydrated in a graded ethanol series, transferred into isoamyl acetate, and dried in a critical point drier (JCPD-5; JEOL) after substitution with liquid CO_2. Dried samples were coated with platinum by using a sputter coater (JFC-1600; JEOL) and were examined under a scanning electron microscope (JSM-5600LV; JEOL) at an accelerating voltage of 10 kV.

Northern Blot Analysis

Total RNA was isolated by using Trizol reagent (Invitrogen) from E9.5 mutant embryos. Northern blot analysis was performed by following standard procedures with full-length *Cthrc1* and *Fzd6* cDNAs as probes. Radioactive signals were detected with a BAS-2500 Bio-Image Analyzer (FujiFilm, Tokyo Japan).

Rho and Rac Activation Assay

HEK293T cells (4×10^5) were seeded in each well of six-well plates. After overnight culture, 0.9 μg expression plasmids was transfected by using FuGENE HD (Roche). For transfection, 500 ng Cthrc1/Cthrc1-ΔC/Cthrc1-ΔGXY and 100 ng Wnt3a/Wnt5a/Dvl2 of pCAGGS-based expression plasmids were used. The amount of transfected DNA was adjusted to 0.9 μg by adding appropriate amounts of the empty vector (pCAGGS). Twenty-four hours after transfection, the cells were lysed, and activation of RhoA and Rac1 was examined with a RhoA and Rac1 activation assay kit (Upstate, VA USA) according to the manufacturer's instructions. The plasmids are described in the Supplemental Data.

Coculture Immunoprecipitation Assay

To prepare protein-expressing cells, HEK293T cells (2×10^6) were seeded in 10 cm dishes for 24 hr, after which the cells were transfected with 4.5 μg pCAGGS-based expression plasmids by using FuGENE HD (Roche). Five hours after transfection, cells were trypsinized and mixed in the ratio described below, and 1×10^6 cells were replated in six-well plates for coculture. Receptor cells and ligand cells were mixed in a ratio of 1:4 to detect the interaction of one receptor and one ligand (Figures 3 and 5). The HA-tagged receptor was immunoprecipitated in all experiments. Similarly, to study the interaction of one receptor and two ligands, a 1:2:2 ratio of receptor:ligand 1:ligand 2 was used (Figures 6A and 6B). To detect the interaction of two receptors and two ligands (Figures 6C and 6D), 2.25 μg of each receptor-expressing plasmid was cotransfected to prepare receptor-expressing cells. The ligand-receptor cell ratio of receptor (1 + 2):ligand 1:ligand 2 was 1:2:2. After 24 hr of coculture, cell lysates were prepared by lysing the cells with 500 μl lysis buffer (50 mM Tris-HCl [pH 8.0], 150 mM NaCl, 1% NP-40, complete protease inhibitor cocktail [Roche]) and removing the insoluble materials by centrifugation at 12,000 × g for 10 min at 4°C. A total of 15 μl of the lysates was used as whole-cell lysates by adding 15 μl 2× SDS sample buffer. The remaining lysates were subjected to immunoprecipitation by incubation with 2 μg anti-HA polyclonal antibody (Y-11; Santa Cruz Biotechnology) at 4°C overnight. Then, 20 μl Protein G Plus-Agarose (Santa Cruz Biotechnology) was added to the lysates, which were further incubated at 4°C for 90 min. Immune complexes were precipitated by centrifugation at 1,000 × g for 2 min, washed four times with 1 ml lysis buffer, and dissolved in 30 μl 2× SDS sample buffer. Immunoprecipitates or whole-cell lysates were separated by SDS-PAGE and blotted onto nitrocellulose membranes (Whatman). Membranes were probed with anti-HA (F-7) (Santa Cruz Biotechnology), anti-myc (9E10) (Santa Cruz Biotechnology), or anti-Flag M2 (Sigma) monoclonal antibodies and were detected by using CDP-Star (Roche). Chemiluminescent signals were detected and quantified by using an LAS-3000 mini lumino image analyzer (FujiFilm). The plasmids are described in the Supplemental Data.

Luciferase Assay

For cotransfection experiments, 1×10^5 HEK293T cells were seeded in 24-well plates 1 day prior to transfection. The cells were transfected with a 250 ng DNA mixture by using FuGENE HD (Roche) and were cultured for 24 hr. The DNA mixture consisted of TOPFLASH reporter (100 ng) (a gift from M. Hibi), pCS2-βgal reference (50 ng) (a gift from M. Hibi), and 100 ng pCAGGS-based effector plasmids. The following amounts of effector plasmids were used: *Wnt3a*, 0.1 ng; *LRP6*, 0.1 ng; *Cthrc1*, 50, 25, and 10 ng; *β-catenin*, 25 ng; and *Dvl2*, 50 ng. The amount of effector DNA was adjusted to 100 ng by addition of an appropriate amount of an empty vector (pCAGGS). Cell lysates were prepared, and luciferase and β-galactosidase activities were measured as described previously (Sasaki et al., 1999). For coculture experiments, 2×10^6 HEK293T cells were seeded per 10 cm dish on the day before transfection. A total of 4.5 μg plasmid DNA was transfected by using FuGENE HD (Roche) to prepare effector and reporter cells. Effector cells were transfected with 4.5 μg pCAGGS-based expression plasmids for *Wnt3a*, *Cthrc1*, and an empty vector (pCAGGS). Reporter cells were transfected with TOPFLASH (500 ng),

pCS2-βgal (250 ng), and pCAGGS (3750 ng). When necessary, pCAGGS-based expression plasmids for Dvl2 (250 ng) and β-catenin (125 ng) were also included, keeping the total DNA amount to 4.5 μg by reducing the amount of pCAGGS. After 5 hr of transfection, reporter and effector cells were trypsinized and mixed in the ratio of 1:2:2 (reporter:effector 1:effector 2) and seeded in 24-well plates. After 24 hr of incubation, luciferase and β-galactosidase activities were measured. Luciferase activities were normalized to β-galactosidase activities. The graphs show the average of two samples with standard errors.

Characterization of Cthrc1

One day before transfection, HEK293T cells (4×10^5) were seeded in six-well plates with 2 ml medium. Cthrc1 expression plasmids (0.9 μg) were transfected by using FuGENE HD (Roche) and were cultured for 24 hr. The medium was used as a conditioned medium, and cell lysate was prepared as in the procedures for coculture IP. Samples were diluted 10-fold, except for the conditioned medium of the N188A mutant. Conditioned medium (2.5 μl) was treated with 1 mU *N*-glycosidase F (Glycopeptidase F, Takara Bio Inc., Shiga, Japan) by following the manufacturer's instructions.

Reverse Transcription-PCR

Total RNAs were isolated from HEK293T cells by using Trizol reagent (Invitrogen) according to the manufacturer's instructions. One microgram of total RNA was used for cDNA synthesis by using Superscript III reverse transcriptase (Invitrogen) according to the manufacturer's instructions. The resulting cDNA was diluted appropriately for semiquantitative PCR. Primers for *Wnt*s, *LRP*s, and *HPRT* were as described by Etheridge et al. (2004), and that for *Ror2* was as described by Oishi et al. (2003). Primers for *Cthrc1* were 5′-TTTCTGGAACCCATGGAGAG-3′ and 5′-AGCCAGCACCTCCTTCTACA-3′. The PCR conditions were 95°C for 1 min; 25, 30, or 35 cycles of 95°C for 30 s; 58°C for 30 s; and 72°C for 1 min, followed by 72°C for 5 min.

SUPPLEMENTAL DATA

Supplemental Data include three figures, Supplemental Experimental Procedures, and Supplemental References and are available at http://www.developmentalcell.com/cgi/content/full/15/1/23/DC1/.

ACKNOWLEDGMENTS

We thank M. Saitou for single-cell cDNA library production protocols, H. Niwa for EB3 ES cells, H. Enomoto for advice on ES cell culture, J.-i. Miyazaki for CAG-CAT-EGFP mice, A. Shimono for loop-tail mutants, T. Sakamoto and H. Togashi for technical advice on dissection of the inner ear, Y. Hayashizaki for FANTOM3 clones, N. Sasai for the JNK assay, and M. Hibi for plasmids. We also thank S. Takada for critical reading of the manuscript. We are also grateful to the Laboratory for Animal Resources and Genetic Engineering for the generation of chimeras and the housing of the mice. This work was supported by grants from RIKEN to H.S.

Received: November 29, 2007
Revised: April 14, 2008
Accepted: May 15, 2008
Published: July 7, 2008

REFERENCES

Dabdoub, A., Donohue, M.J., Brennan, A., Wolf, V., Montcouquiol, M., Sassoon, D.A., Hseih, J.C., Rubin, J.S., Salinas, P.C., and Kelley, M.W. (2003). Wnt signaling mediates reorientation of outer hair cell stereociliary bundles in the mammalian cochlea. Development *130*, 2375–2384.

DeChiara, T.M., Kimble, R.B., Poueymirou, W.T., Rojas, J., Masiakowski, P., Valenzuela, D.M., and Yancopoulos, G.D. (2000). Ror2, encoding a receptor-like tyrosine kinase, is required for cartilage and growth plate development. Nat. Genet. *24*, 271–274.

Durmus, T., Leclair, R.J., Park, K.S., Terzic, A., Yoon, J.K., and Lindner, V. (2006). Expression analysis of the novel gene collagen triple helix repeat containing-1 (Cthrc1). Gene Expr. Patterns *6*, 935–940.

Etheridge, S.L., Spencer, G.J., Heath, D.J., and Genever, P.G. (2004). Expression profiling and functional analysis of wnt signaling mechanisms in mesenchymal stem cells. Stem Cells *22*, 849–860.

Greene, N.D., Gerrelli, D., Van Straaten, H.W., and Copp, A.J. (1998). Abnormalities of floor plate, notochord and somite differentiation in the loop-tail (Lp) mouse: a model of severe neural tube defects. Mech. Dev. *73*, 59–72.

Habas, R., and Dawid, I.B. (2005). Dishevelled and Wnt signaling: is the nucleus the final frontier? J. Biol. *4*, 2.

Habas, R., Kato, Y., and He, X. (2001). Wnt/Frizzled activation of Rho regulates vertebrate gastrulation and requires a novel Formin homology protein Daam1. Cell *107*, 843–854.

Habas, R., Dawid, I.B., and He, X. (2003). Coactivation of Rac and Rho by Wnt/Frizzled signaling is required for vertebrate gastrulation. Genes Dev. *17*, 295–309.

Hikasa, H., Shibata, M., Hiratani, I., and Taira, M. (2002). The *Xenopus* receptor tyrosine kinase Xror2 modulates morphogenetic movements of the axial mesoderm and neuroectoderm via Wnt signaling. Development *129*, 5227–5239.

Jones, C., and Chen, P. (2007). Planar cell polarity signaling in vertebrates. Bioessays *29*, 120–132.

Katoh, M. (2005). WNT/PCP signaling pathway and human cancer. Oncol. Rep. *14*, 1583–1588.

Katoh, M., and Katoh, M. (2007). WNT signaling pathway and stem cell signaling network. Clin. Cancer Res. *13*, 4042–4045.

Kawamoto, S., Niwa, H., Tashiro, F., Sano, S., Kondoh, G., Takeda, J., Tabayashi, K., and Miyazaki, J. (2000). A novel reporter mouse strain that expresses enhanced green fluorescent protein upon Cre-mediated recombination. FEBS Lett. *470*, 263–268.

Kibar, Z., Vogan, K.J., Groulx, N., Justice, M.J., Underhill, D.A., and Gros, P. (2001). Ltap, a mammalian homolog of *Drosophila* Strabismus/Van Gogh, is altered in the mouse neural tube mutant Loop-tail. Nat. Genet. *28*, 251–255.

Kishida, S., Yamamoto, H., and Kikuchi, A. (2004). Wnt-3a and Dvl induce neurite retraction by activating Rho-associated kinase. Mol. Cell. Biol. *24*, 4487–4501.

Labus, M.B., Stirk, C.M., Thompson, W.D., and Melvin, W.T. (1998). Expression of Wnt genes in early wound healing. Wound Repair Regen. *6*, 58–64.

LeClair, R.J., Durmus, T., Wang, Q., Pyagay, P., Terzic, A., and Lindner, V. (2007). Cthrc1 is a novel inhibitor of transforming growth factor-β signaling and neointimal lesion formation. Circ. Res. *100*, 826–833.

Liu, G., Bafico, A., and Aaronson, S.A. (2005). The mechanism of endogenous receptor activation functionally distinguishes prototype canonical and noncanonical Wnts. Mol. Cell. Biol. *25*, 3475–3482.

Logan, C.Y., and Nusse, R. (2004). The Wnt signaling pathway in development and disease. Annu. Rev. Cell Dev. Biol. *20*, 781–810.

Mikels, A.J., and Nusse, R. (2006). Purified Wnt5a protein activates or inhibits β-catenin-TCF signaling depending on receptor context. PLoS Biol. *4*, e115.

Montcouquiol, M., Rachel, R.A., Lanford, P.J., Copeland, N.G., Jenkins, N.A., and Kelley, M.W. (2003). Identification of Vangl2 and Scrb1 as planar polarity genes in mammals. Nature *423*, 173–177.

Murdoch, J.N., Doudney, K., Paternotte, C., Copp, A.J., and Stanier, P. (2001). Severe neural tube defects in the loop-tail mouse result from mutation of Lpp1, a novel gene involved in floor plate specification. Hum. Mol. Genet. *10*, 2593–2601.

Neidhardt, L., Gasca, S., Wertz, K., Obermayr, F., Worpenberg, S., Lehrach, H., and Herrmann, B.G. (2000). Large-scale screen for genes controlling mammalian embryogenesis, using high-throughput gene expression analysis in mouse embryos. Mech. Dev. *98*, 77–94.

Nishita, M., Yoo, S.K., Nomachi, A., Kani, S., Sougawa, N., Ohta, Y., Takada, S., Kikuchi, A., and Minami, Y. (2006). Filopodia formation mediated by receptor tyrosine kinase Ror2 is required for Wnt5a-induced cell migration. J. Cell Biol. *175*, 555–562.

Niwa, H., Masui, S., Chambers, I., Smith, A.G., and Miyazaki, J. (2002). Phenotypic complementation establishes requirements for specific POU domain and generic transactivation function of Oct-3/4 in embryonic stem cells. Mol. Cell. Biol. *22*, 1526–1536.

Oishi, I., Suzuki, H., Onishi, N., Takada, R., Kani, S., Ohkawara, B., Koshida, I., Suzuki, K., Yamada, G., Schwabe, G.C., et al. (2003). The receptor tyrosine kinase Ror2 is involved in non-canonical Wnt5a/JNK signalling pathway. Genes Cells *8*, 645–654.

Park, M., and Moon, R.T. (2002). The planar cell-polarity gene stbm regulates cell behaviour and cell fate in vertebrate embryos. Nat. Cell Biol. *4*, 20–25.

Pinson, K.I., Brennan, J., Monkley, S., Avery, B.J., and Skarnes, W.C. (2000). An LDL-receptor-related protein mediates Wnt signalling in mice. Nature *407*, 535–538.

Pyagay, P., Heroult, M., Wang, Q., Lehnert, W., Belden, J., Liaw, L., Friesel, R.E., and Lindner, V. (2005). Collagen triple helix repeat containing 1, a novel secreted protein in injured and diseased arteries, inhibits collagen expression and promotes cell migration. Circ. Res. *96*, 261–268.

Qian, D., Jones, C., Rzadzinska, A., Mark, S., Zhang, X., Steel, K.P., Dai, X., and Chen, P. (2007). Wnt5a functions in planar cell polarity regulation in mice. Dev. Biol. *306*, 121–133.

Sasaki, H., Nishizaki, Y., Hui, C., Nakafuku, M., and Kondoh, H. (1999). Regulation of Gli2 and Gli3 activities by an amino-terminal repression domain: implication of Gli2 and Gli3 as primary mediators of Shh signaling. Development *126*, 3915–3924.

Shimizu, H., Julius, M.A., Giarre, M., Zheng, Z., Brown, A.M., and Kitajewski, J. (1997). Transformation by Wnt family proteins correlates with regulation of β-catenin. Cell Growth Differ. *8*, 1349–1358.

Slusarski, D.C., Corces, V.G., and Moon, R.T. (1997). Interaction of Wnt and a Frizzled homologue triggers G-protein-linked phosphatidylinositol signalling. Nature *390*, 410–413.

Takada, R., Hijikata, H., Kondoh, H., and Takada, S. (2005). Analysis of combinatorial effects of Wnts and Frizzleds on β-catenin/armadillo stabilization and Dishevelled phosphorylation. Genes Cells *10*, 919–928.

Takeuchi, S., Takeda, K., Oishi, I., Nomi, M., Ikeya, M., Itoh, K., Tamura, S., Ueda, T., Hatta, T., Otani, H., et al. (2000). Mouse Ror2 receptor tyrosine kinase is required for the heart development and limb formation. Genes Cells *5*, 71–78.

Tamai, K., Semenov, M., Kato, Y., Spokony, R., Liu, C., Katsuyama, Y., Hess, F., Saint-Jeannet, J.P., and He, X. (2000). LDL-receptor-related proteins in Wnt signal transduction. Nature *407*, 530–535.

Tang, L., Dai, D.L., Su, M., Martinka, M., Li, G., and Zhou, Y. (2006). Aberrant expression of collagen triple helix repeat containing 1 in human solid cancers. Clin. Cancer Res. *12*, 3716–3722.

Veeman, M.T., Axelrod, J.D., and Moon, R.T. (2003a). A second canon. Functions and mechanisms of β-catenin-independent Wnt signaling. Dev. Cell *5*, 367–377.

Veeman, M.T., Slusarski, D.C., Kaykas, A., Louie, S.H., and Moon, R.T. (2003b). Zebrafish prickle, a modulator of noncanonical Wnt/Fz signaling, regulates gastrulation movements. Curr. Biol. *13*, 680–685.

Wang, J., Mark, S., Zhang, X., Qian, D., Yoo, S.J., Radde-Gallwitz, K., Zhang, Y., Lin, X., Collazo, A., Wynshaw-Boris, A., et al. (2005). Regulation of polarized extension and planar cell polarity in the cochlea by the vertebrate PCP pathway. Nat. Genet. *37*, 980–985.

Wang, J., Hamblet, N.S., Mark, S., Dickinson, M.E., Brinkman, B.C., Segil, N., Fraser, S.E., Chen, P., Wallingford, J.B., and Wynshaw-Boris, A. (2006a). Dishevelled genes mediate a conserved mammalian PCP pathway to regulate convergent extension during neurulation. Development *133*, 1767–1778.

Wang, Y., Guo, N., and Nathans, J. (2006b). The role of Frizzled3 and Frizzled6 in neural tube closure and in the planar polarity of inner-ear sensory hair cells. J. Neurosci. *26*, 2147–2156.

Yabuta, Y., Kurimoto, K., Ohinata, Y., Seki, Y., and Saitou, M. (2006). Gene expression dynamics during germline specification in mice identified by quantitative single-cell gene expression profiling. Biol. Reprod. *75*, 705–716.

Ybot-Gonzalez, P., Savery, D., Gerrelli, D., Signore, M., Mitchell, C.E., Faux, C.H., Greene, N.D., and Copp, A.J. (2007). Convergent extension, planar-cell-polarity signalling and initiation of mouse neural tube closure. Development *134*, 789–799.